Resolution in Column Chromatography of Polymer Latexes. I. The Light Scattering Behavior of Polystyrene and Its Effect on Signal Resolution in HDC

D. J. NAGY,* C. A. SILEBI, and A. J. MCHUGH,** *Departments of Chemistry and Chemical Engineering and Emulsion Polymers Institute, Lehigh University, Bethlehem, Pennsylvania 18015*

Synopsis

A method for improving signal resolution in latex particle-size analysis by HDC is presented and discussed. Data for the extinction cross section and specific extinction coefficient for polystyrene latex standards indicate that improvements in signal resolution can be obtained for the small particle end of broad size distributions by using turbidity detection at wavelengths less than 254 nm. Data are also discussed for the imaginary refractive index of the polystyrene standards obtained from comparisons of the extinction cross section results with Mie theory calculations. HDC runs made with bimodal and continuous distributions at 254 and 220 nm wavelength detection are also discussed to illustrate the improvements in size distribution resolution which can result.

INTRODUCTION

Application of the techniques of packed column chromatography to the size analysis of colloidal sols in the submicron range is a relatively recent development. The method, developed by Small,[1,2] involves closed columns packed with nonporous beads through which a dilute latex suspension is pumped and is referred to as Hydrodynamic Chromatography, or HDC. The name derives from the fact that the separation mechanism is a single-phase flow process involving fractionation as a result of a size-dependent interaction between the stabilized colloidal particles and eluant velocity gradients in the packing interstices. Previous publications have presented complete analyses of the convected flow separation model[3–7] which describes well the role of the principal parameters in the separation process. Methods for calculating particle size distribution directly from the output chromatogram, using variations on the techniques developed for size exclusion chromatography, have also been thoroughly discussed.[8,9] In the latter two articles, theoretical calculations, based on the Mie theory for light scattering, indicated that improvements in HDC signal resolution could result by using turbidity detection at wavelengths where the latex particles absorb as well as scatter.

An important practical aspect of the development of HDC is the consideration of methods for optimizing resolution. In this article, attention will be directed to the light scattering behavior of polystyrene latex particles to show the effects

* Current address: Air Products and Chemicals, Allentown, PA 18105.

** Author to whom correspondence should be addressed. Current address: Department of Chemical Engineering, University of Illinois, Urbana, IL 61801.

Journal of Applied Polymer Science, Vol. 26, 1555–1565 (1981)
 CCC 0021-8995/81/051555-11$01.10

of signal resolution on the separation capabilities of the technique. A companion article (part II) will present a comparison of the column resolution characteristics of porous and nonporous packing systems.

LATEX DETECTION AND SIGNAL RESOLUTION

Latex detection in HDC is normally carried out turbidimetrically at a fixed wavelength in the UV range; and, depending on the light scattering characteristics of the latex system, the resulting signal will be due to either pure scattering or scattering plus absorption. Owing to the relatively small values of λ/D_p (wavelength to particle diameter ratio), the signal depends strongly on particle diameter as well as concentration and chemistry. This is in contrast to size exclusion chromatography of dissolved macromolecules, in which differential refractometry is the currently preferred detection method. Since the output signal in this case depends only on concentration and not on molecular size, molecular weight analysis from the output chromatogram is greatly simplified.[10,11] The extensive use of refractive index monitors is additionally favored by the high sensitivity of the detection signal in the range of polymer concentrations normally used in size exclusion analysis.

The use of differential refractometry in HDC has also been reported.[8,9,12,13] Experimental measurements on static systems indicate that the refractive index signal will be proportional to the particle suspension weight fraction in the normal range of particle sizes encountered in HDC.[8,9] Analysis of the signal detection characteristics also indicates that relative signal intensity over the normal particle size range (several hundred angstroms to several thousand angstroms diameter) is more nearly uniform compared to the turbidity calculation for pure scattering.[9] Since broad continuous particle-size distributions are often the norm in latex production, uniform signal resolution over the entire size range is an important consideration. Algorithms presented in ref. 9 also demonstrate clearly that the highly nonlinear relationship between turbidity and particle size, for a purely scattering system, profoundly influences accuracy and numerical stability of the calculations for particle size distribution. A major drawback to the use of differential refractometry in HDC however, is the need for increased particle concentrations due to lower instrument sensitivity to particle detection. This often leads to column clogging or material balance problems.[9,14] In addition, commercially available instruments can change from positive to negative signal outputs for different particle sizes as well as give baseline instability with slight temperature variations.[14]

For light scattering, the relationship between turbidity τ and extinction cross section R_{ext} can be written as

$$\tau = NR_{ext}x \tag{1}$$

where N is the number of particles per unit volume and x is the optical path length. Calculations in ref. 9, for a range of particle diameters using Mie theory to evaluate R_{ext} as a function of imaginary refractive index, show that the signal for small particles will be enhanced by absorption while that for the larger particles slightly decreases. The first feature suggests better detection of smaller particles, while the second feature results in a relative signal for large to small particles which is superior to that predicted for refractometry. Since, as indi-

cated, lower particle concentrations are possible with turbidimetric detection, it would appear to be the preferred method. Thus, a more detailed experimental analysis of the wavelength dependence of latex light scattering and its effect on HDC signal resolution has been carried out and will be reported in the following sections.

EXPERIMENTAL

Turbidity measurements were made using a variable-wavelength UV photometer. Suspensions of Dow monodisperse polystyrene standards (discussed elsewhere[3]) were used along with polystyrene latex labeled #LS-1166 B (particle diameter 1.10 μm, standard deviation 0.006 μm) and one labeled #LS-1117B (diameter 794 nm, standard deviation 0.0044 μm). Solutions were diluted to various concentration ranges in deionized water. Each sample was referenced to deionized water, and optical density was recorded for wavelengths between 200 and 350 nm for each concentration.

Chromatography runs, to be reported, were made using the HDC instrument and technique fully described elsewhere.[1,3] The system consists of three columns packed with 20-μm-diam styrene–divinylbenzene copolymer beads, through which eluant (deionized water plus surfactant) is pumped at a flow rate of 0.6 ml/min. The surfactant used was either sodium lauryl sulfate or sodium dihexylsulfosuccinate (aerosol MA) and was added to an ionic strength of $1.0 \times 10^{-3}M$. Particle suspensions passed from the columns through a variable-wavelength, flow-through detector.

EXTINCTION DATA FOR POLYSTYRENE

For the experimental measurement of R_{ext} latex concentrations are generally based on gravimetric determinations. Thus, eq. (1) is written as

$$\tau = \left(\frac{\rho_{12}}{\rho_2}\right)\left(\frac{\phi_m}{v_p}\right) R_{ext} x \tag{2}$$

where v_p is the particle volume, ϕ_m is the suspension mass fraction, and ρ_2 and ρ_{12} are the latex sphere and suspension densities, respectively. For a fixed particle diameter, the slope of the optical density–weight fraction plot can be used with eq. (2) to determine R_{ext}. For the smallest particles (88-nm standard) some deviation from linearity was observed at very low concentrations at 220-nm wavelength, as shown in Figure 1. The same plot shows that as particle size was increased (234 nm in this case), a linear dependence, consistent with eq. (1), resulted. Nonlinearities could be the result of photometer saturation or multiple particle absorption effects and indicate the need for low particle concentrations in the HDC analysis. (Column injection samples, to be reported later, were limited to 0.005 wt % latex, since an additional dilution by a factor of 10 occurs during flow through the columns.[3])

The specific extinction coefficient gives a measure of relative signal intensity between various particle populations at a given wavelength. The expression for the coefficient k_{ext} is

$$k_{ext} = \left(\frac{\rho_{12}}{\rho_2}\right)\frac{R_{ext}}{2.303 v_p} \tag{3}$$

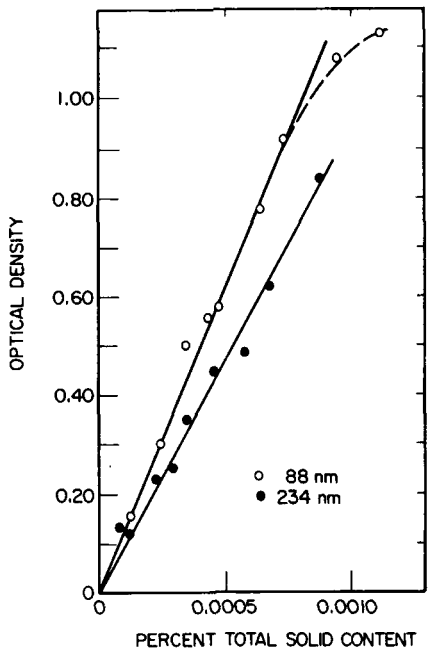

Fig. 1. Concentration dependence of the turbidimetric signal for monodisperse 88- and 234-nm polystyrene standards at 220-nm wavelength.

Figure 2 shows a plot of k_{ext} versus wavelength for the various polystyrenes and illustrates clearly that for the 38- and 109-nm standards a strong signal enhancement occurs at wavelengths less than 254 nm. The 176- and 357-nm-diameter standards show less enhancement below 254-nm wavelength, in line with the calculations in ref. 9. Figure 3 more clearly shows the comparison of relative weight signal versus particle size for an absorbing (220 nm) and nonabsorbing (254 nm) wavelength (comparison of calculated scattering cross sections with measured cross sections at 254 nm in ref. 9 demonstrated pure scattering occurs for polystyrene latexes at this wavelength). The strong dependence of signal intensity with particle size at 254 nm reflects the nature of pure scattering

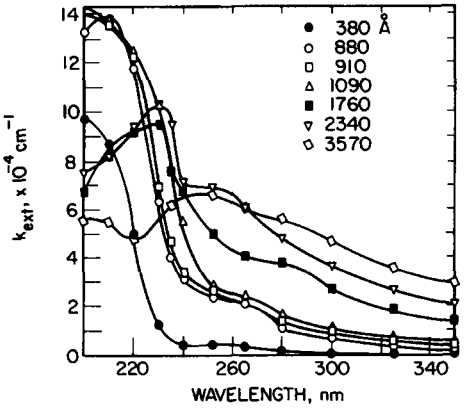

Fig. 2. Experimental dependence of the specific extinction coefficient for polystyrene standards from 88- to 357-nm diam.

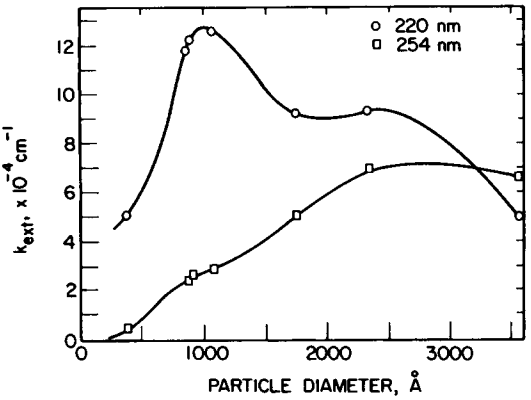

Fig. 3. Experimental dependence for polystyrene of the specific extinction coefficient on particle size for wavelengths of 220 and 254 nm.

behavior. The difficulty in accurately detecting small numbers of small particles at this wavelength is indicated, for example, by the ratio of k_{ext} values for the 234- and 38-nm particles of approximately 16. On the other hand, at 220 nm, the signal intensity for the small particles increases and the relative k_{ext} values improve, e.g., the ratio for the 234- to 38-nm signals is now approximately 1.8.

For the calculation of weight-averaged size distributions, an ideal detection system would show a third power dependence on particle size. At a given wavelength, the extinction cross section for a series of monodisperse standards can be approximated by a power law relation.[15] Thus, we can write

$$R_{ext} \propto D_p^k \tag{4}$$

where k is the power law exponent (strictly speaking the turbidity averaged exponent.) Figure 4 shows an example of a typical fit of our data to a power law

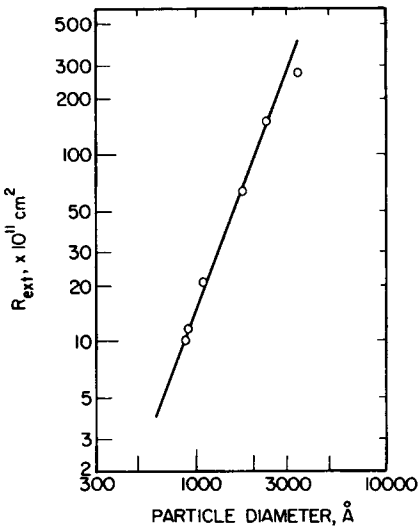

Fig. 4. Experimental extinction cross section vs. particle diameter at 220-nm wavelength–logarithmic coordinates.

relationship; these data are for the 220-nm wavelength. Figure 5 shows the wavelength dependence of the power law exponent derived from the slopes of the log R_{ext}–log D_p plots. The break which occurs in the curve around 240 nm indicates the probable borderline between pure scattering (above 240 nm) and combined scattering and absorption. In terms of signal sensitivity, the power law exponent of 4 at 254 nm gives a further indication of the relative signal problems encountered in the size distribution analyses previously reported.[9] At 220 nm, the exponent is roughly 2.7, which indicates possible improvement in signal resolution for a broadly distributed polydisperse system. For an ideal weight-averaged signal, similar to size-exclusion refractometry, a third power dependence on D_p is needed and is indicated from these data to occur at 227 nm.

DETERMINATION OF THE IMAGINARY REFRACTIVE INDEX

The algorithms in ref. 9 for particle size distribution from the HDC chromatogram are based on Mie theory calculations for the turbidity signal. In order to analyze size distribution data in the absorbing wavelength range, additional data for the imaginary part of the complex refractive index are required. Alternately, a more empirical approach using eq. (4) directly in the chromatogram analysis can be developed. Such an approach has been discussed by Hamielic and Singh.[16] In this section the results for extinction cross section will be converted to values for the complex refractive index. In the next section, these results will be applied to HDC chromatographic data for several polydisperse systems.

The general expression for R_{ext} from Mie theory can be written[15] as

$$R_{ext} = \frac{\lambda^2}{2\pi} \sum (2n + 1)\,\mathrm{Re}(a_n + b_n) \tag{5}$$

In eq. (5), the coefficients a_n and b_n are functions of the refractive index of the medium and of the particle, m_p, as well as the dimensionless wave number α (= $\pi D_p/\lambda$) and Re represents the real part of the sum. For wavelength regions where the particles can absorb radiation as well as scatter, m_p, is written as

$$m_p = m_1 - im_2 \tag{6}$$

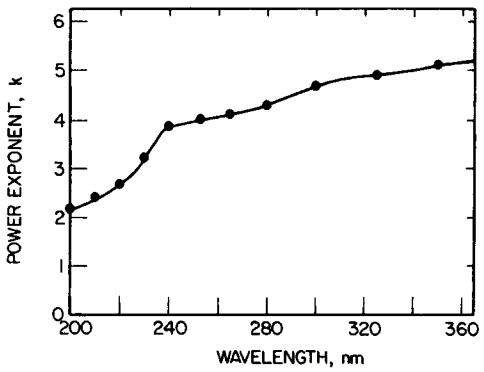

Fig. 5. Power law exponent of particle diameter for polystyrene as function of wavelength for particle diameters 88–357 nm.

where m_1 and m_2 are, respectively, the real and imaginary parts of the refractive index. For nonabsorbing particles, m_2 is zero, and it increases as the wavelength of an absorption peak is reached.

Best values of m_2 for polystyrene can be obtained by fitting eq. (5) to the R_{ext} data for various assumed m_2. Previous calculations[9] have shown that Mie theory accurately predicts the scattering cross section, R_{scat}, for polystyrene. As a consequence of the strong functionality of R_{ext} with m_2 in the small-particle region ($D_p < 176$ nm), the determination of the best value was made by comparison between calculated and measured R_{ext} in this size range.[14]

Table I lists the m_2 values obtained, and Figure 6 shows these data along with results reported by Carter et al.[17] and Partridge.[18] These results clearly show that absorption in polystyrene occurs for wavelengths less than 240 nm. The data of ref. 17 were obtained from reflectance measurements and indicate absorption due to $\pi \rightarrow \pi^*$ transitions of the polystyrene aromatic rings. Reflectance measurements are inherently less accurate than direct absorption mea-

TABLE I
Values for the Imaginary Part of the Complex Refractive Index of Polystyrene Latexes

Wavelength, nm	m_2
200	0.50
210	0.59
220	0.48
230	0.18
240	0.04
254	0.02
265	0.006
280	0
300	0
325	0
350	0

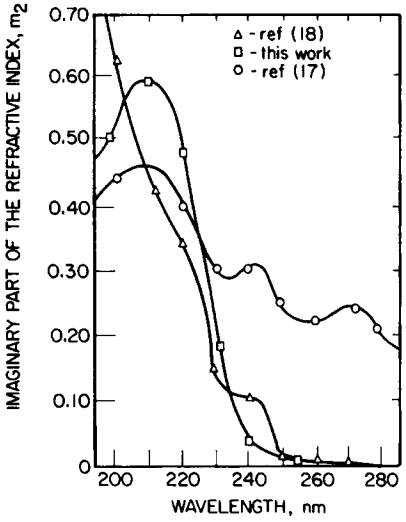

Fig. 6. Comparison of experimental values for the imaginary part of the complex refractive index for polystyrene to the data of Carter et al.[17] and Partridge.[18]

surements, especially in regions of low absorption (small m_2), and would indicate false absorption for polystyrene at wavelengths greater than 254 nm. The data of Partridge, however, were obtained from spectrophotometric measurements and are similar to those obtained by Bush and Weinreb[19] for wavelengths between 110 and 230 nm. In contrast to the results of Carter, Partridge's absorption spectrum indicates that polystyrene exhibits only very weak absorption above 240 nm and is transparent at longer wavelengths. Partridge found that at shorter wavelengths, where absorption is much greater, Carter's reflectance measurements do follow the general shape of the direct absorption curve. Our experimental results for the polystyrene latexes agree well with the data of Partridge and indicate very weak absorption at 254 nm, while below 240 nm polystyrene is a strongly chemical absorbing species. Values for the imaginary part of the complex refractive index can be used to compute extinction, absorption, and scattering cross sections over the wavelength range of 200–300 nm for particle sizes of 380–3570 Å. Results of such calculations are presented elsewhere[14] and show the same trends in behavior seen in the k_{ext} results discussed here.

SIGNAL RESOLUTION AND HDC

The application of these results to improved HDC resolution was first tested by chromatographing a series of mixtures of several different standards through the HDC system with detection at 220 and 254 nm. Figure 7 shows the results for a 1.00–1.20 weight mixture of the 38- and 176-nm standards. Despite a ratio of particle numbers greater than 80:1, only a small shoulder shows at 254 nm, indicating the presence of the 38-nm population. At 220 nm, the relative peak heights (as well as signal intensity) are dramatically improved, indicating clearly the bimodal nature of the system. Similar results were seen for a 1.07/1.00 (8.6/1 by number) biomodal mixture of the 88- and 176-nm standards and a 1.00/7.36 (1.1/1.0 by number) mixture of the same. The relative signal enhancement in

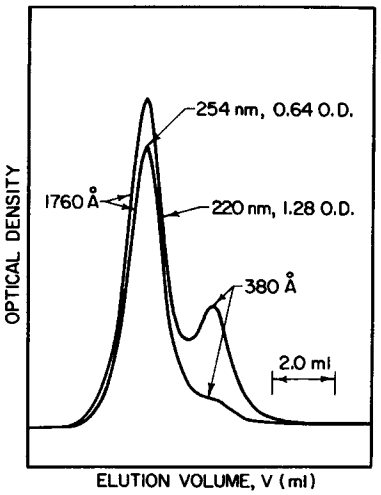

Fig. 7. Optical density HDC chromatograms for biomodal mixture, 1.00/1.20 by weight, of 38- and 176-nm polystyrene standards, at 254- and 220-nm detector wavelength.

the latter two cases was less than that shown in Figure 7; however, in both cases the biomodal nature of the mixture was more clearly apparent at 220 nm than at 254 nm.[14]

The ultimate application of improved signal resolution is, of course, for the complete size distribution analysis for a polydisperse system. For a continuous distribution, the relationship between the measured chromatogram, $F(V)$, and the true chromatogram, $W(y)$, corrected for dispersion, is given by[8,9]

$$F(V) = \int_{V_1}^{V_2} G(V,y)\, W(y)\, dy \tag{7}$$

In eq. (7), $G(V,y)$ is the normalized instrument spreading function for the particle size with mean retention volume y, and the integral is evaluated over the chromatogram limts V_1 to V_2. The conversion of $W(y)$ to the total number of a given particle size, $N_T(y)$, is given by the integrated form of eq. (1):

$$N_T(y) = \frac{2.303 W(y)}{x R_{\text{ext}}(y)} \tag{8}$$

Solution of eqs. (7) and (8) requires an approximation for the spreading function $G(V,y)$, along with sufficient input data to calculate R_{ext} from Mie theory. A complete discussion of various techniques for solving eqs. (7) and (8) is given in ref. 9. The modified Ishige, Lee, and Hamielic method discussed in ref. 9 was used to analyze several HDC runs at 254 and 220 nm detector wavelengths. Briefly, the algorithm is an iterative method which starts with a first estimate of $W(y)$ obtained from the polydisperse chromatogram assuming no axial dispersion. Equation (7) is then solved numerically, using data from the chromatograms for the various monodisperse standards to approximate $G(V,y)$ yielding a computed chromatogram $F^*(V)$. Subsequent iterations correct $W(y)$ according to the error between the computed and measured chromatograms. The correction is given by

$$W_i^{j+1} = W_i^j \prod_{k=-n}^{n} \left(\frac{F_{i+k}^*}{F_{i+k}}\right)^{\alpha} \tag{9}$$

where j refers to the level of iteration. The quantity α is a weighting coefficient taken from the actual contributions to F_{i+k} of the neighboring particle sizes within $\pm 2\sigma$ of the elution volume of interest, where σ is the standard deviation

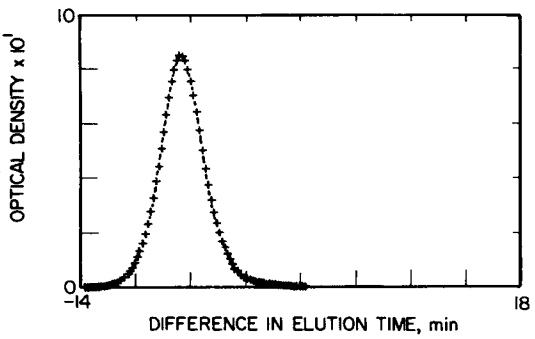

Fig. 8. Experimental (−) and calculated (+) chromatogram for 2D2 latex with 29%, 38 nm standard at 254 nm detector wavelength.

or second moment of the chromatogram. The number of symmetric terms, n, about F_{i+k} is chosen according to the spread in the chromatogram.[9]

As an illustration of the role of signal wavelength on resolution, results are shown in Figures 8–10 for several HDC runs. A polydisperse polystyrene latex (labeled 2D2), to which 29% by number of a 38-nm-diam Dow standard was added, was chromatographed under standard conditions in both cases, except for the choice of detector wavelength. Figures 8 and 9 show, respectively, the chromatogram fit and comparison between the normalized chromatographic size distribution and that measured by electron microscopy. These data are similar to results shown earlier[9] and indicated that at 254 nm, despite a close chromatogram fit, a marked mismatch between calculated and measured size distribution occurs in the small particle region. For the same system, chromatographed under identical conditions, except for the detector signal which was 220 nm, a similar close fit of the chromatogram resulted. Figure 10 shows, however, a marked improvement in the size distribution calculation.

The algorithm for the analysis uses a linear equation for the ln D_P–V relationship, the slope of which is used in the size distribution normalization.[9] In actual fact, for particles less than 50 nm in diameter, the ln D_p–V calibration curve begins to approach the origin in a nonlinear fashion.[14] Details of a power law curve fitting method for the non-linear portion of the calibration curve are

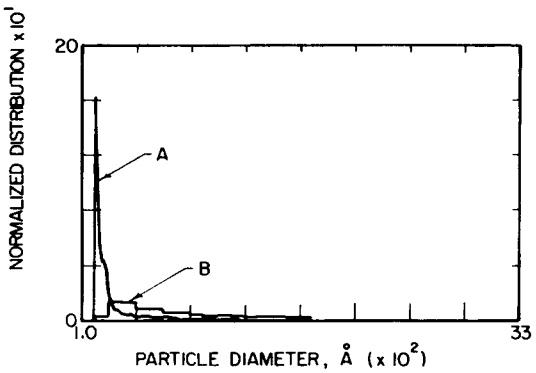

Fig. 9. Calculated particle size distribution (solid curve) and measured distribution (histogram) from Fig. 8.

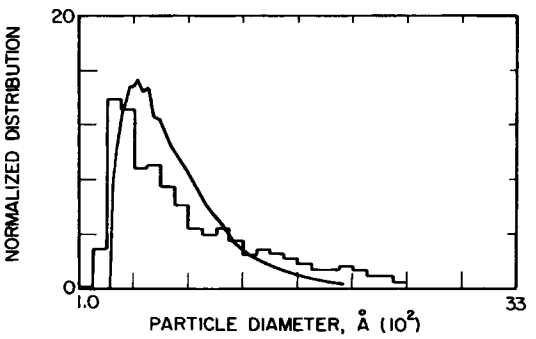

Fig. 10. Calculated particle size distribution (solid curve) and measured distribution (histogram) for latex of Fig. 8 run at 220 nm detector wavelength.

given in ref. 14. Since the 38-nm particle calibration point falls in the nonlinear region, one might expect improved accuracy in the size distribution analysis from such an approach. However, the agreement between calculated and measured size distributions, for both wavelengths, turned out to be less than that shown here for the linear calibration assumption. This points to the added sensitivity of the calculation to the calibration curve slope in the small particle region. Nonetheless, the relative improvement in the size distribution calculation at 220 nm as compared to 254 nm, seen here, also resulted.[14]

The net conclusion of these results is that signal wavelength can play an important role in optimizing the resolution of HDC size analysis, particularly if one is dealing with a broad size distribution. Algorithms developed previously, in combination with complex refractive index measurements for the latex in question, can be used to evaluate optimum wavelength for a given system.

This work has been carried out under a grant from the National Science Foundation (ENG 77-07041), along with funds from the Industrial Liaison Program of the EPI. One of the authors (D.N.) has also received partial support from a Lever Brothers Company Foundation Fellowship.

References

1. H. Small, *J. Colloid Interface Sci.*, **48**, 147 (1974).
2. H. Small, F. L. Saunders, and J. Solc, *Adv. Colloid Interface Sci.*, **6**, 237 (1976).
3. R. F. Stoisits, G. W. Poehlein, and J. W. Vanderhoff, *J. Colloid Interface Sci.*, **57**, 337 (1976).
4. A. J. McHugh, C. A. Silebi, G. W. Poehlein, and J. W. Vanderhoff, *Colloid Interface Science*, Vol. IV, Academic, New York, 1976, p. 549.
5. C. A. Silebi and A. J. McHugh, *AChE J.*, **24**, 204 (1978).
6. D. C. Prieve and P. M. Hoysan, *J. Colloid Interface Sci.*, **64**, 201 (1978).
7. B. A. Buffham, *J. Colloid Interface Sci.*, **67**, 154 (1978).
8. C. A. Silebi and A. J. McHugh, in *Emulsions, Latices, and Dispersions*, P. Becher and M. N. Yudenfreund, Eds., Marcel Dekker, New York, 1978, pp. 155–174.
9. C. A. Silebi and A. J. McHugh, *J. Appl. Polym. Sci.*, **23**, 1699 (1979).
10. C. F. Simpson, Ed., *Practical High Performance Liquid Chromatography*, Heyden and Son, New York 1976, pp. 174–176.
11. F. W. Billmeyer, *Textbook of Polymer Science*, 2nd ed., Wiley–Interscience, New York, 1971, pp. 52–56.
12. H. Coll and G. R. Fague, *J. Colloid Interface Sci.*, **76**, 116 (1980).
13. S. Singh and A. E. Hamielic, *J. Appl. Polym. Sci.*, **22**, 577 (1978).
14. D. J. Nagy, Ph.D. thesis, Lehigh University, May 1979.
15. M. Kerker, *The Scattering of Light and Other Electromagnetic Radiation*, Academic, New York, 1969.
16. A. E. Hamielic and S. Singh, *J. Liq. Chromatogr.*, **1**(2), 187 (1978).
17. J. G. Carter, T. M. Jelinek, R. N. Hamm, and R. D. Birkhoff, *J. Chem. Phys.*, **44**, 2266 (1966).
18. R. H. Partridge, *J. Chem. Phys.*, **47**, 4223 (1967).
19. L. Bush and A. Weinreb, Argonne National Laboratory, Summary Report ANL-6326, March 1961.

Received August 29, 1980
Accepted October 5, 1980